J. Ind. Geophys. Union (October 2007)
Vol.11, No.4, pp.189-196

A new approach to seismic diffraction tomography technique and its significance in ore-body prospecting

Mahasweta Mahapatra and Samiran Mahapatra
Department of Geology, Durgapur Government College, Durgapur - 713 214
E-mail: mahasweta_mahapatra@rediffmail.com

ABSTRACT

Diffraction, once considered noise rather than signal in seismic tomography, has recently been successfully used in ore-body prospecting, particularly in delineating smaller objects which otherwise cannot be properly investigated by ray tomography methods.

Most prevalent seismic diffraction tomography techniques use Born's approximation of weak scattering instead of considering total wave field. In the present study, using total scattered wave field, at first, the forward modeling for objects of different geometrical shapes and sizes, both separately and in combination is done and then very fast simulated annealing is employed for inverse modeling. Subsequently, annealing parameters are used to determine the model parameters such as size, contrast and distance of the object from measuring plane. This gives fairly good estimate for model parameters within acceptable error limit.

This procedure of seismic diffraction tomography technique can potentially be used for investigating ore-body of smaller dimension having not only weak but also strong scattering properties.

INTRODUCTION

Until recently diffraction tomography has received little weightage in the field of mineral prospecting and has generally been considered noise rather than signal in seismic tomography techniques. However, in the last few decades diffraction tomography has gained momentum particularly in delineating the smaller objects which otherwise cannot be properly investigated by ray tomography methods. To paraphrase Bleistein (1984), if the largest wavelength found in band limited data is λmax, then the ray approximation is valid when the anomalies are of the order of $3\lambda max$ or larger.

Most prevalent seismic diffraction tomography techniques (Devaney, 1982, 1984; Wu & Toksöz, 1987; Lo et al., 1988; Lo, Duckworth & Toksöz, 1990; Naidu et al., 1995) used Born's approximation of weak scattering instead of considering the total wave-field. But there are many geological objects like ore-shoots in hydrothermal ore deposits, kimberlite-lamproite intrusions and karst objects which are not weak but strong scatterers. These objects may not be properly investigated using the approach based on Born's approximation of weak scattering. In the present study, total wave-field of scattered wave has been considered in delineating blind ore-bodies of smaller dimension and the technique is applicable to both weak as well as strong scatterers.

METHODOLOGY

The problem of seismic diffraction tomography has been divided into two parts: i) Forward modeling ii) Inverse modeling. At first, in the forward modeling, synthetic scattered field data has been generated for smaller objects of different geometrical shapes. For simplicity, however, we concentrate on 2D cases only. The synthetic data thus generated have then been used for inverse modeling using very fast simulated annealing (VFSA) technique. Fig.1 shows a generalized flow diagram of the steps required to solve the problem.

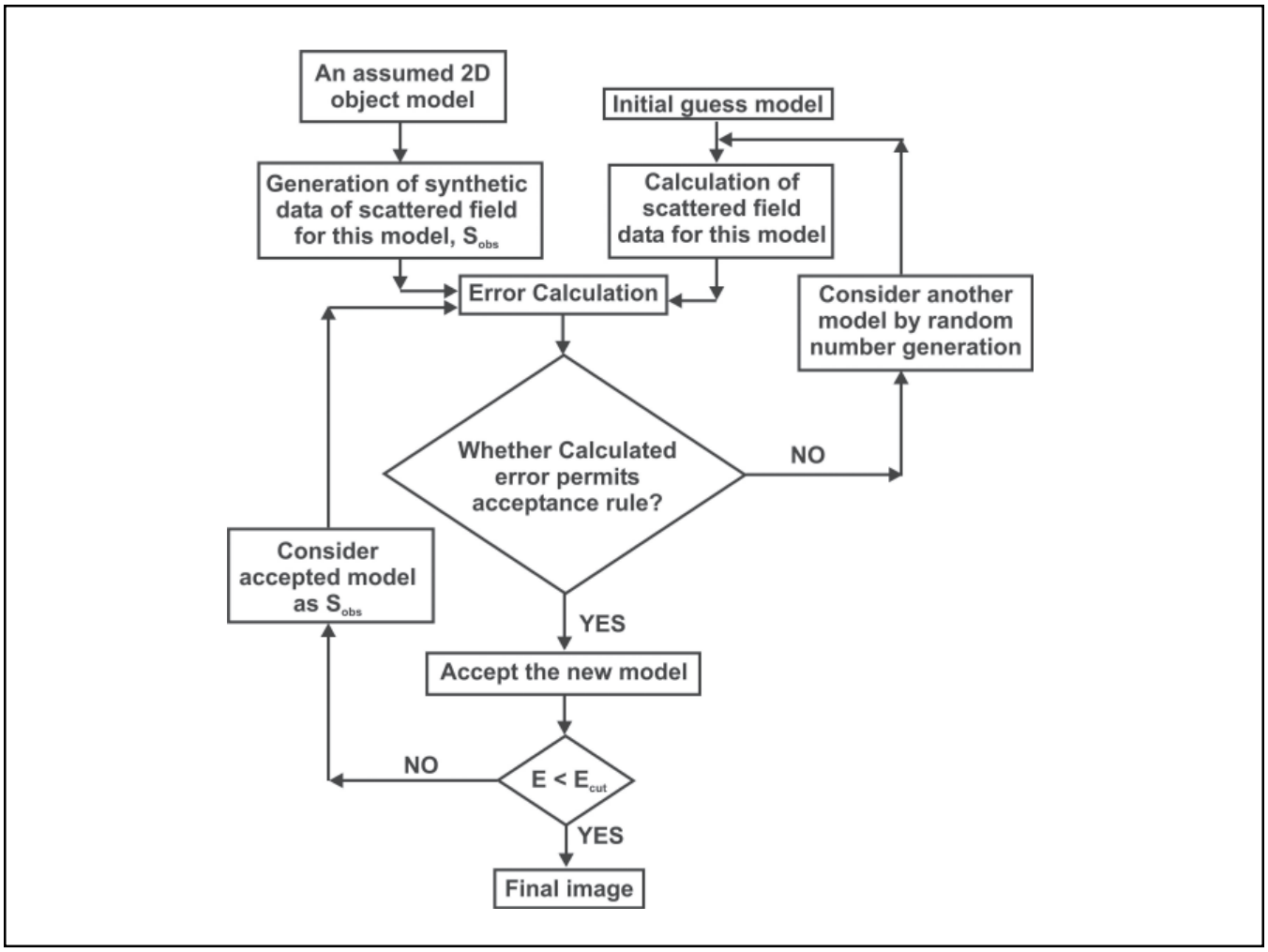

Figure 1. Generalized flow diagram showing steps of diffraction tomography.

FORWARD MODELING

Diffraction has its origin in geometrical optics and has similarities in its implementation to seismic tomography. Consequently, the scattered field data have been calculated using the exact solution developed in geometrical optics (Francon 1966) without considering any approximation.

Synthetic data have been generated for different types of models such as rectangle, square, circle and ellipse. Fig. 2 shows the geometrical setup for the data acquisition. However, some assumptions have been made during the forward modeling. The object of the refractive index contrast n has been considered to be embedded in a homogeneous medium. The source is considered as plane wave of single frequency and multiple scattering has been avoided.

Forward modeling for square/rectangular object has been done by using equation:

$$U(x, y) = (4abn/\lambda_0) \{Sin (k_0nla) / (k_0nla)\} \{sin (k_0nmb) / (k_0nmb)\} \ldots (i)$$

Where U(x, y) is the scattered field measured at a point (x, y), a and b are the length and width of the object, n is the refractive index contrast, l = x/R, m = y/R, R is the perpendicular distance between the object plane and the measuring plane, $k_0 = 2\pi/\lambda_0$, λ_0 is the wavelength of the incident wave. By changing the sizes it has been found that scattering effect is dominant for the objects whose size is comparable to the wavelength of the incident wave. Otherwise, for large scale objects, however, most of the energy of the incident wave gets reflected and/or refracted.

Forward modeling for circular objects of different radius and refractive index contrast has been done using equation:

$$U(x, y) = \{(2\pi a^2.n) /\lambda_0\} \{J_1 (k_0na\alpha) / (k_0na\alpha)\} \ldots (ii)$$

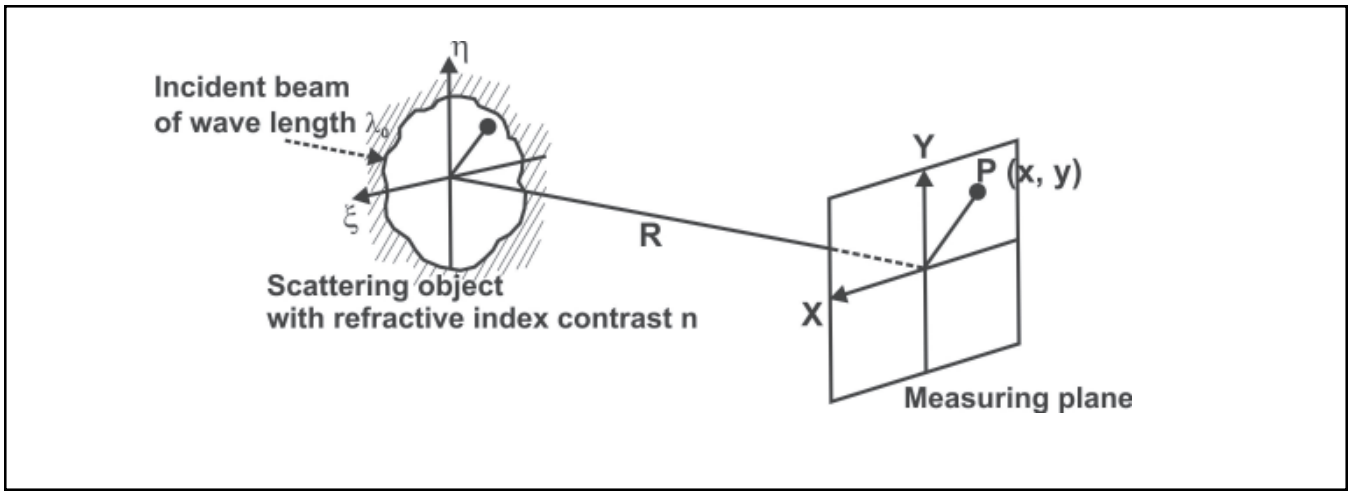

Figure 2. Geometrical set up for data acquisition.

Where U(x, y) is the scattered field measured at a point (x, y), a is the radius of the object, n is the refractive index contrast, $k = (2\pi) / \lambda_0$, λ_0 is the wavelength of the incident wave, $\alpha = (l^2 + m^2)^{1/2}$, $l = x / R$, $m = y / R$; R is the distance between the object plane and the measuring plane and J_1 is the Bessel function of 1st order.

A generalized expression for the scattered field of an elliptical object has been developed by the equation:

$$U(x, y) = \{(2\pi ab.n) /\lambda_0\} \{J_1 (k_0 n\alpha') / (k_0 n\alpha')\} \quad \ldots \text{(iii)}$$

Where, U(x, y) is the scattered field measured at a point (x, y), a = Major axis of the ellipse, b = Minor axis of the ellipse, $\alpha' = (l^2a^2 + m^2b^2)^{1/2}$. Forward modeling for circular objects as a special case of elliptical object is also tested. For a circle, a = b, $\alpha' = a (l^2 + m^2)^{1/2} = a\alpha$, and the equation (iii) leads to: $U(x, y) = \{(2\pi a^2.n) /\lambda_0\} \{J_1 (k_0 na\alpha) / (k_0 na\alpha)\}$, which is same as equation (ii).

INVERSE MODELING

The problem of diffraction tomography satisfies nonlinear equation. In most of the cases this has been solved by using Fourier Diffraction Theorem in frequency domain. However, in the present work, VFSA method (Ingber 1993; Chunduru, Sen & Stoffa 1997) is considered as the inversion technique. The advantage of the VFSA technique is that it can jump out of local minima and can achieve the global minimum. Another advantage is that the starting model need not be close to the global minimum which can be of great help in real earth problem. Here, the dimension of the object, distance of the object from the measuring plane and the refractive index contrast are taken as unknown parameters.

RESULTS WITH SYNTHETIC DATA

Though the geological features may be of any shapes, emphasis has been given on regular geometrical shape of ellipse since many other shapes can be represented by combinations of ellipses and/or its variant circles.

The scattered field due to an elliptical object with refractive index contrast 0.01 with the surrounding media has been measured by using equation (iii). The wavelength of the incident wave is taken as 0.01 and the length of the major and minor axis of the elliptical object is taken as 0.6 λ_0 and 0.12 λ_0 respectively. The field has been measured on a plane at a perpendicular distance of 35 λ_0 from the object. Fig. 3 shows the graphical representation of the distance vs. scattered field plot. These synthetic data are then inverted by VFSA method to obtain the unknown model parameters. Starting from an initial temperature 10^5, 2000 iterations have been carried out with a cooling schedule as given in equation:

$$T_i = T_0 \exp \{-\text{decay}^{*}(i-1)^{0.5}\} \quad \ldots \text{(iv)}$$

Where, T_0 is the starting temperature for model, T_i is the temperature in the i^{th} iteration and the decay value is taken as 0.97 which is found to be optimum in the present case.

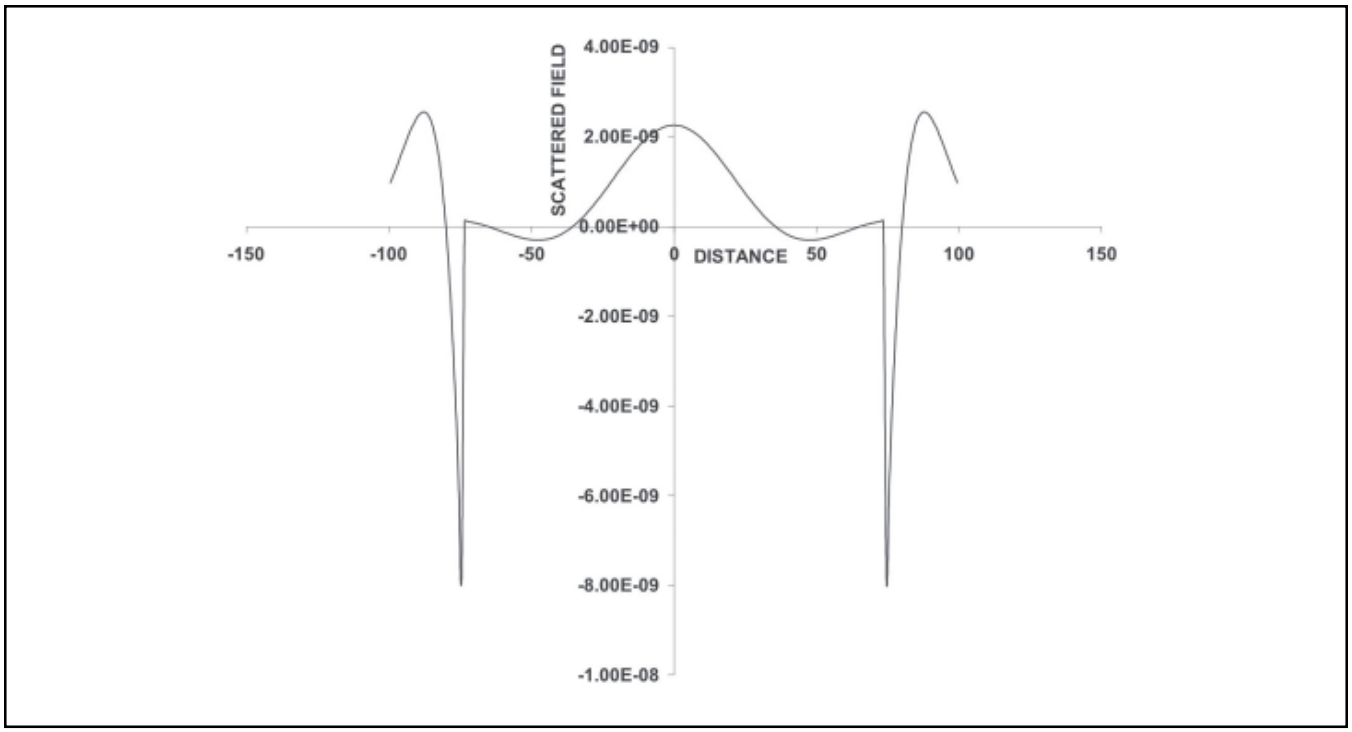

Figure 3. Graphical representation of synthetic scattered field data for elliptical model.

Model parameter	Minimum	Maximum	Increment
t_1	0.40	0.80	0.01
t_2	0.10	0.30	0.01
t_3	30.00	40.00	0.50
n	0.005	0.05	0.001

Table. 1. Search window and search increments for the model parameters of the elliptical model. Here, $t_1 = a/\lambda_0$, $t_2 = b/a$, $t_3 = R/\lambda_0$.

Representative error for each iteration has been calculated by different methods like least-square, root mean square, standard deviation and weighted average method. Among these, weighted (with respect to corresponding observed data obtained from forward model) average method gives the best result for the inversion. The search window and search increments for the parameters are shown in Table 1. Fig. 4 represents the iteration vs. error plot for this operation and it is clear from the figure that global minimum has been achieved after 500 iterations. The model parameters obtained are as follows: lengths of the major and minor axis are $0.62\lambda_0$, $0.18\lambda_0$ respectively, Distance of the object from the measuring plane is $35.16\lambda_0$ and the refractive index contrast is 0.009. Graphical representation showing comparison between the actual and calculated model are given in Fig. 5.

This method has also been tested on the models of square, rectangular and circular shape. The results obtained are shown in Table 2. with the actual values given in parentheses.

After considering the smaller objects of different shapes separately, the method developed here is also tested in delineating objects in combination, such as an elliptical object and a rectangular object, embedded in a homogeneous medium. The combined scattered field has been obtained by summing the individual scattered field of each model. This combined field is then inverted by VFSA technique. The guess parameters used and the results obtained are given in Tables.3 and 4 respectively.

Table. 2. Results after VFSA inversion for circular, rectangular and square objects.

Model	Size	R	n
Circular	Radius, $0.72\lambda_0$ ($0.6\lambda_0$)	$30.65\lambda_0$ (35.00_0)	0.009 (0.01)
Rectangular	$0.44\lambda_0$ x $0.18\lambda_0$ ($0.60\lambda_0$ x $0.30\lambda_0$)	$38.50\lambda_0$ ($35.00\lambda_0$)	0.012 (0.01)
Square	$0.47\lambda_0$ x $0.69\lambda_0$ ($0.6\lambda_0$ x $0.6\lambda_0$)	$37.19\lambda_0$ ($35.00\lambda_0$)	0.010 (0.01)

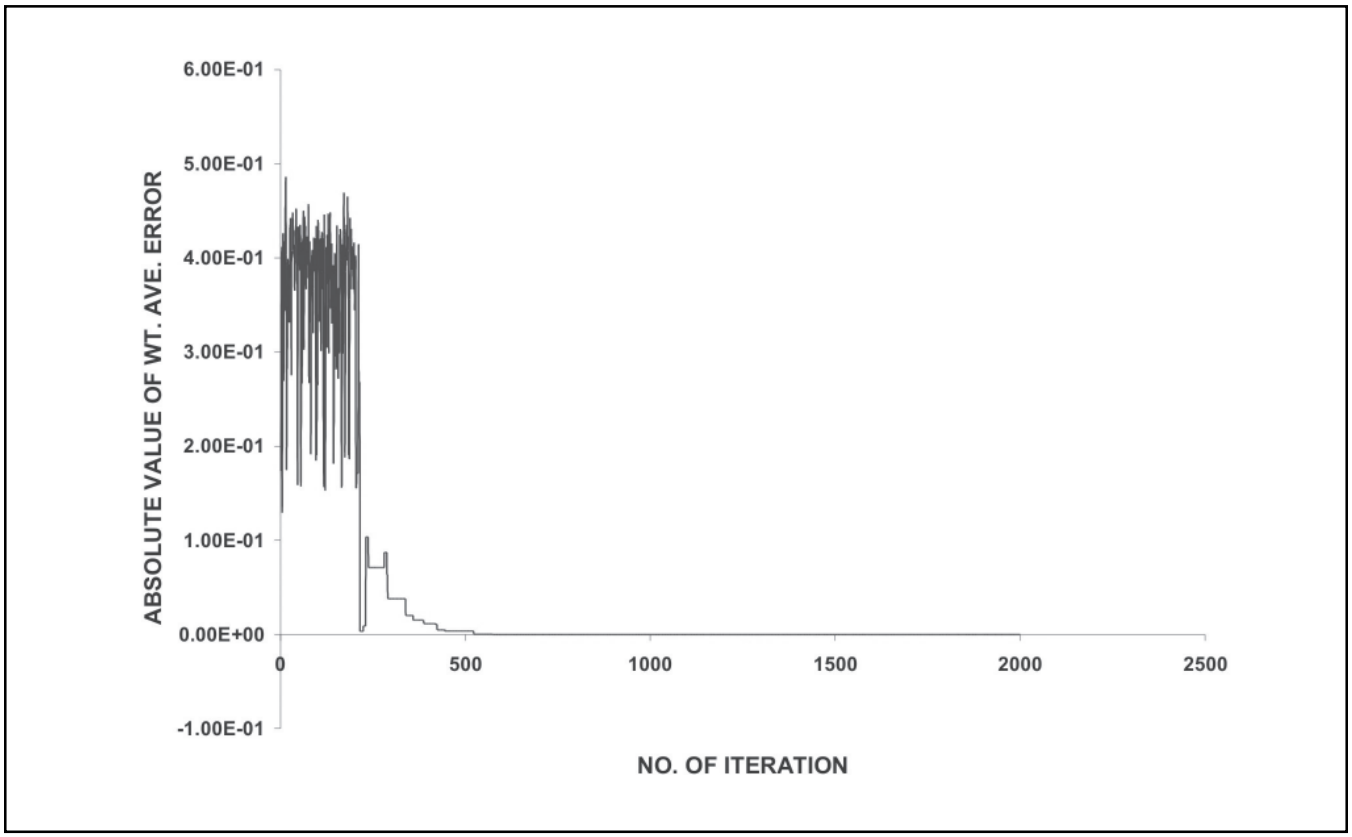

Figure 4. Iteration vs. absolute value of weighted average error plot during the nonlinear optimization technique for elliptical model.

Table. 3. Guess parameters for the combined model. Here, $t_1 = a/\lambda_0$, $t_2 = b/a$, $t_3 = R/\lambda_0$.

Parameter	Minimum		Maximum		Increment	
	Ellipse	Rectangle	Ellipse	Rectangle	Ellipse	Rectangle
t_1	0.10	0.10	2.00	2.00	0.01	0.01
t_2	0.05	0.05	1.00	1.00	0.01	0.01
t_3	10.00	10.00	80.00	80.00	1.00	1.00
n	0.001	0.001	0.05	0.05	0.001	0.001

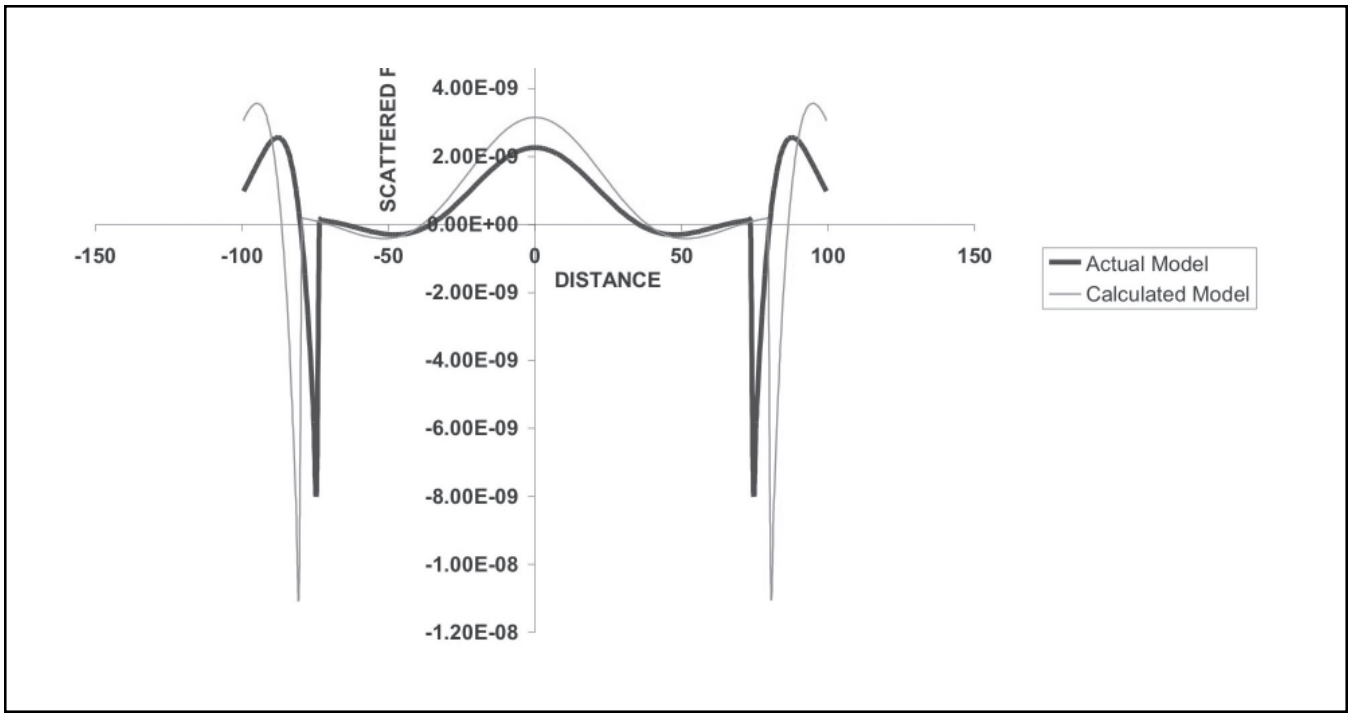

Figure 5. Comparison between scattered field of the actual and calculated model for an elliptical object.

Table. 4. Results after VFSA inversion for the model having combination of elliptical and rectangular objects. Figures in the parentheses are the actual values.

Object	Size	R	n
Elliptical	$0.78\lambda_0 x 0.27\lambda_0$ ($0.6\lambda_0 x 0.12\lambda_0$)	$36.43\lambda_0$ ($35.00\lambda_0$)	0.01 (0.01)
Rectangular	$0.82\lambda_0 x\, 0.19\lambda_0$ ($0.80\lambda_0 x\, 0.40\lambda_0$)	$55.60\lambda_0$ ($50.00\lambda_0$)	0.03(0.03)

DISCUSSION

In this paper, we have demonstrated a nonlinear optimization technique applied to synthetic seismic scattered field data for objects of smaller dimension having different sizes and shapes, both separately and in combination. The algorithm of the generation of scattered field for these objects and the inversion technique has been developed. However, in forward modeling instead of conventional Born's approximation of weak scattering the total wavefield is considered. This allows the approach to be valid also for large-scale scatterers and thus more appropriate to tackle the exploration of blind ore bodies of smaller dimension. Inverse modeling is carried out by using VFSA technique since, unlike the technique using Fourier Diffraction Theorem, it is less sensitive to sampling geometry (Sevink & Herman 1994). The enumerated seismic diffraction tomography method gives fairly good estimate for model parameters within acceptable error limit. However, some estimated parameters give aberrant values. This can be controlled by proper assumption of search limits (guess values) supplemented by other geological information of the concerned area. This procedure of seismic diffraction tomography technique can potentially be used for investigating mineral deposits where the ore-shoots in the host rock (e.g. hydrothermal ore deposits) or the host itself (e.g. diamondiferous kimberlite-lamproite intrusions) are small enough to be delineated by traditional ray tomography methods. In some hydrothermal deposits the ore minerals are found to be concentrated along some suitable locales of small aerial extent, like veins, fissures, hinges of the associated folds (McGowan et al., 2003), cave and collapse structures formed by karstification in

Mississippi valley type deposits (Olson 1984) etc. Kimberlite-lamproite intrusions with characteristic weak velocity contrast and vertical orientation may create problems in identification by ray tomography method particularly, if it is covered by high velocity layer (in case of refraction tomography) or in absence of convenient reflection boundary below the pipe body (in case of reflection tomography). Such objects of small aerial extent are, however, strong scatterers and, consequently, can easily be delineated by the seismic diffraction tomography technique dealt with here.

ACKNOWLEDGEMENTS

This paper is an offshoot of the project SR/ WOS-A/ ES-47/ 2003 funded by DST, Govt. of India, under Women Scientist Scheme. The financial assistance received for the project from DST is gratefully acknowledged. The authors are also thankful to the Principal, Durgapur Govt. College, Durgapur, for providing the necessary infrastructural facilities. The authors would like to specially acknowledge the benefit of interaction they had with Sri Mahendra Dutta, Assistant Professor in Mathematics, Durgapur Govt. College, Dr. R.K.Shaw, Assistant professor and Dr. P.R.Mohanty, Associate Professor, Dept. of Applied Geophysics, Indian School of Mines, Dhanbad, who extended unstinted support and shared with the authors their personal view on subjects of their specialization. The authors are also grateful to the anonymous reviewers of the Journal for their critical and constructive reviews and suggestions that have substantially improved the manuscript.

REFERENCES

Bleistein, N., 1984. Mathematical methods for wave phenomenon, Academic Press, New York, p.18.

Chunduru, R.K., Sen, M.K. & Stoffa, P.L., 1997, Hybrid optimization methods for geophysical inversion, Geophysics, 62 (4), 1196-1207.

Devaney,A.J., 1982. A filtered back-propagation algorithm for diffraction tomography, Ultrasonic Imaging, 4, 336-350.

Devaney,A.J., 1984. Geophysical diffraction tomography, IEEE Transactions on Geoscience and Remote Sensing, 22, 3-13.

Francon, M., 1966. Diffraction coherence in optics, Pergamon Press Ltd., Oxford, 137p.

Ingber, L., 1993. Simulated Annealing: Practice verses Theory, Journal of Mathematical Computation Modelling, 18 (11), 29-57.

Lo, T., Duckworth, G.L. & Toksöz, M.N., 1990. Minimum cross entropy seismic diffraction tomography, J. Acoust. Soc. Am., 87 (2), 748-756.

Lo, T., Toksöz, M.N., Xu, S. & Wu, R.S., 1998. Ultrasonic laboratory tests of geophysical tomographic reconstruction, Geophysics, 53, 947-956.

McGowan, R.R., Roberts, S., Foster, R.P., Boyce, A.J. & Coller, D., 2003. Origin of the copper-cobalt deposits of the Zambian Copperbelt: An epigenetic view from Nchanga, Geology, 31 (6), 497-500.

Naidu, P.S., Vasuki, A., Satyamurthy, P. & Anand, J., 1995. Diffraction tomographic imaging with a circular array, IEEE Trans. On Ultrasonics, Ferroelectrics and Frequency Control, 42 (4), 883-885.

Olson, R.A., 1984. Genesis of paleokarst and strata-bound zinc-lead sulfide deposits in a Proterozoic dolostone, Northern Baffin Island, Canada, Economic Geology, 79, 1056-1103.

Sevink, A.G.J. & Herman, G.C., 1994. Fast iterative solution of sparsely sampled seismic inverse problems, Inverse Problems, 10, 937-948.

Wu,R.S. & Toksöz, M.N., 1987. Diffraction tomography and multisource holography applied to seismic imaging, Geophysics, 52, 11-25.

(Accepted 2007 August 21. Received 2007 August 16; in original form 2007 November 6)

Ms. Mahasweta Mahapatra did her graduation with Physics Honours from B.B.College, Asansol, Burdwan district, West Bengal in 1990. She then obtained her M.Sc. Tech. degree in Applied Geophysics and M.Tech. degree in Petroleum Exploration from Indian School of Mines, Dhanbad in 1994 and 1995 respectively. She is presently working as project scientist in a project under women scientist scheme, DST, Government of India, at Durgapur Govt. College, Durgapur, West Bengal. Her area of interest is in seismic tomography.

Dr. Samiran Mahapatra was born in January, 1967 in Durgapur, Burdwan district, West Bengal. The author's school and early college education was in Durgapur. Then he studied in Indian School of Mines, Dhanbad and obtained his M.Sc. Tech. degree in Applied Geology and M.Tech degree in Mineral Exploration in 1992 and 1993 respectively. He has obtained Ph.D. degree in Geology from The University of Burdwan in 2004. He is now serving as Lecturer (Sr.scale) in Geology in Durgapur Government College, Durgapur, West Bengal. His research interest is in sedimentology.